Electrochimica Acta 56 (2011) 4445–4450

Contents lists available at ScienceDirect

Electrochimica Acta

journal homepage: www.elsevier.com/locate/electacta

Electrochemical and UV–Vis/ESR spectroelectrochemical properties of thienylenevinylenes substituted by a 4-cyanostyryl group

M. Czichy[a,*], A. Stolarczyk[a], P. Wagner[b], W. Domagala[a], M. Lapkowski[a,c], D.L. Officer[b]

[a] Department of Physical Chemistry and Technology of Polymers, Silesian University of Technology, 9 ks. M. Strzody Str., 44-100 Gliwice, Poland
[b] Intelligent Polymer Research Institute and ARC Centre of Excellence for Electromaterials Science, University of Wollongong, Northfields Avenue, Wollongong, NSW 2522, Australia
[c] Centre of Polymer and Carbon Materials, Polish Academy of Sciences, 34 M. Sklodowska-Curie Str., 41-819 Zabrze, Poland

ARTICLE INFO

Article history:
Received 31 August 2010
Received in revised form 1 February 2011
Accepted 4 February 2011
Available online 24 February 2011

Keywords:
Thienylenevinylenes
Styryl group
Electropolymerisation
UV–Vis
ESR

ABSTRACT

The π-electron delocalisation in conjugated thienylenevinylenes bearing arylethenyl chromophores, makes those materials interesting candidates for electro-optic applications. In this study, we report the results of electrochemical and UV–Vis/ESR spectroelectrochemical studies of a pair of thienylenevinylenes substituted by the 4-cyanostyryl group, bearing either a hydrogen, or methyl group terminated α carbons at the peripheral thiophene rings. The reactivity of various functional segments of investigated molecules was assessed by comparing the reactivity of the protected and unprotected counterparts and the behaviour of their electrooxidation products. For the capped derivative, two irreversible anodic redox processes giving electrochemically inactive products were observed, while the uncapped molecule yields electroactive materials already upon its first oxidation step.

1. Introduction

Organic conjugated polymers with extensive π-electron delocalisation are the topic of great interest for numerous optoelectronic and photonic applications [1–3]. Most notably, the energy spacing between the frontier occupied and unoccupied orbitals (the band gap) is often appropriate for UV–Vis driven electron excitation leading to generation of excitons. On account of this advantageous property conjugated polymers show great promise as the semiconducting layer in devices such as polymer light emitting diodes (PLEDs), organic field effect transistors (OFETs) and organic photovoltaic cells (OPV). Moreover such semiconducting layers are lightweight, flexible, with anticipated manufacturing costs being lower than for conventional inorganic semiconductors [4,5].

Conjugated polymers such as polythiophenes (PTs), polypyrroles (PPy), poly(*p*-phenylenevinylene)s (PPVs) and their derivates are extensively employed as light harvesting and hole-transport materials for photovoltaic devices, due to their high absorption coefficients in the visible part of electromagnetic spectrum, high mobility of charge carriers and excellent stability [6,7]. The introduction of side-chains to these polymers modulates their intermolecular forces leading to lessening of rigidity and agglomeration strength. While this leads to improvement of solubility and fusibility, both of which facilitate processing steps [8,9], such macromolecular functionalisation can detriment electrical properties quite notably. In spite of these benefits and pitfalls, polymers with side-chain chromophore groups are preferably employed as light absorption materials, facilitating generation and separation of excitons into holes and electrons, and promoting transport of generated holes and electrons to the electrodes. For this reason, our interest encompasses polymers bearing a styryl group, being considered as active components of organic solar cells with large open-circuit voltage [10–12].

The band gap (E_g) and frontier orbital energy levels of the π-conjugated polymers are of crucial importance for photovoltaic devices. For single and hetero junction cells, a band gap of ca. 1.4 eV or 1.3–1.9 eV in general, is being considered optimal [13–15]. Introduction of substituents alters the electric and optical properties of the polymeric material, broadening and shifting its absorption spectrum. It is known for example, that grafting electron-withdrawing groups on the polythiophene backbone results in a decrease of HOMO and LUMO levels [16,17]. For the exciton generation process, it is very important that the absorption spectrum of the active layer match that of the solar spectrum, thus chemists have synthesised many low band gap and broad absorption polymers like thienylenevinylenes (PTV)s, to harvest more photons at long wavelengths. These class of polymers exhibit a lower band gap (1.55–1.8 eV) than polythiophenes together with a stiffer polymer backbone [18,19]. Distortion problems arise however upon side group introduction, as a result of steric interaction

* Corresponding author. Tel.: +48 32 237 17 36.
E-mail address: Malgorzata.Czichy@polsl.pl (M. Czichy).

0013-4686/$ – see front matter © 2011 Elsevier Ltd. All rights reserved.
doi:10.1016/j.electacta.2011.02.019

between thiophene rings and substituent entities. In the case of 3′-styryl-2,2′:5′,2″-terthiophene, the torsion angle between the central and outer thiophene ring, closest to the alkene linker, is −148.6° and the corresponding angle on the opposite side of the central thiophene ring is −151.2° [20]. Despite advantages of PTV, the vinyl bonds in conjugated polymers (PPVs, PTVs) were reported susceptible to oxidation and charge trapping, all which can lead to degradation of the material and deterioration of its electrochemical properties [21,22].

In this study we have employed electrochemistry and UV–Vis/ESR spectroelectrochemistry methods to investigate the progress of polymerisation, chemical stability of thienylenevinylenes and their electroxidation products.

2. Experimental

The monomers: 3-[(*E*)-2-(4-cyanophenyl)ethenyl]-2,5-bis[(*E*)-2-thien-2-ylethenyl]-thiophene (**A**); 3-[(*E*)-2-(4-cyanophenyl)ethenyl]-2,5-bis[(*E*)-2-(5-methylthien-2-yl)ethenyl]-thiophene (**B**) were synthesised in a multistep synthesis, reported previously [23]. The exact structures of monomers are depicted in Scheme 1.

Cyclic voltammetry experiments (CV) were conducted on an AUTOLAB PGSTAT20 potentiostat–galvanostat (EcoChemie). The working and counter electrodes were both platinum wires. Pseudo-Ag/Ag^+ reference electrode was used, hence ferrocene/ferrocenium was employed as a reference redox couple. Before experiments, the electrolyte solutions were deaerated with argon. Electropolymerisation was carried out from 1×10^{-3} M solution of a monomer using cyclic voltammetry at potential sweep rate of 0.05 V s^{-1}. The electrolyte was 0.1 M Bu_4NBF_4 in dry acetonitrile. The compounds were used without additional purification.

Spectroelectrochemical measurements were performed using Cintra 5 UV–Vis spectrophotometer (GBC Scientific Equipment Ptd Lpt). The measurements were performed *in situ* in potentiostatic mode by means of a Cypress 2000 potentiostat. The working electrode was an ITO quartz plate from Delta Technologies, Stillwater, MN, U.S.A. The quasireference electrode and the counter electrode were as described above.

In situ ESR measurements were performed using B-ER-418 Bruker X-band CW spectrometer operating at 100 kHz modulation, coupled together with a Cypress 2000 potentiostat. To avoid microwave saturation, ESR spectra were acquired at low microwave power of 2.1 mW (attenuation of 15 dB) (*M*). First derivative ESR spectra have been recorded for all studied samples and the following parameters of resonance lines were analyzed: *g*-factor, amplitude (*A*), integral intensity (*I*), and linewidth (ΔB_{pp}). The *g*-values were calculated from resonance condition according to the formula [24]: $g = h\nu/\mu_B B_r$, where: h – Planck constant, ν – microwave frequency, μ_B – Bohr magneton, B_r – resonance magnetic field. Microwave frequency (ν) was measured directly by a frequency meter. Additionally, microwave saturation studies in the range of 0.7–63.0 mW powers were carried out to evaluate the spin–lattice relaxation processes in the samples studied.

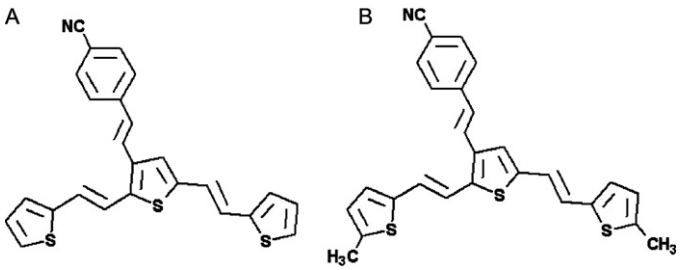

Scheme 1.

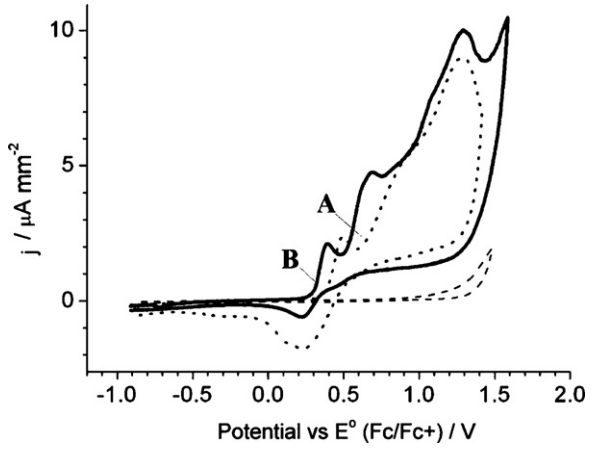

Fig. 1. 1st cycle voltammogram of oxidation of **A** (···) and **B** (▬) in 0.1 M Bu_4NBF_4 solution in acetonitryle (- - -), at Pt electrode. Potential sweep rate: 0.05 V s^{-1}.

The line shape of the ESR signal of **B**'s electrooxidation products was studied using numerical algorithm given by Opfermann [25]. Attempts were made to approximate the experimental spectra by different superposition of Gauss and Lorentz curves. As the best results of curve fitting, those approximations which gave the smallest value of root-mean-square deviation were assumed. The parameters of the best-fit lines: linewidth (ΔB_{pp}), *g*-factor and abundances of component groups of paramagnetic centres, whose lines made up the total spectrum, were evaluated. Contribution of each component to the experimental spectrum of the studied samples was also evaluated. Concentration of paramagnetic centres is proportional to the integral intensity (*I*) of ESR line [24,26]. The integral intensities were calculated by two-step integration of first-derivative ESR spectra.

3. Results and discussion

Fig. 1 presents the cyclic voltammograms of **A** and **B**. The first oxidation peaks correspond to creation of radical cations of both compounds i.e.: $[\mathbf{A}]^{\bullet+}$ at 0.49 V and $[\mathbf{B}]^{\bullet+}$ at 0.39 V. Subsequent peak of **B** response at 0.65 V is attributed to subsequent oxidation of **B** to dication. An amalgamation of oxidation peaks culminating at ca. 1.3 V represents higher oxidation steps of both compounds whose irreversible nature points to high instability of these moieties resulting in their subsequent degradation.

During the first cycle, the scanning potential was restricted to values just past the oxidation peak. Reverse half-cycle of **A** shows, that the first oxidation step is irreversible. Instead we observed the reduction peaks of polymerisation products at 0.03 V and 0.36 V (Fig. 2a). This observation together with the absence of distinct redox couples of **A** at higher potentials indicates a high reactivity of $[\mathbf{A}]^{\bullet+}$. Contrary to these observations, two redox couples of B can be distinguished, the first couple being more reversible than second one (Fig. 2 b and c). All oxidation processes however are semi-reversible.

The ratio of currents of the first and second anodic peak of **B** amounts to 1.7. Being greater than one, this suggests that the second oxidation signal comprises not only oxidation of a radical cation to dication, but also other electrode reactions taking place at these potentials. Despite α-Me substitution, the voltammogram shows that the radical cation and dication are reactive species undergoing consecutive chemical reactions. Repetitive potential cycling of **B** solution in the potential range of both anodic redox steps affords reproducible voltammograms, as a consequence of which, formation of polymer film on the electrode surface is not observed, but instead, blue coloured soluble oxidation products can